

Article

Preparation of Polysilsesquioxane-Based CO₂ Separation Membranes with Thermally Degradable Succinic Anhydride and Urea Units

Katsuhiro Horata ¹, Tsubasa Yoshio ¹, Ryuto Miyazaki ¹, Yohei Adachi ¹ , Masakoto Kanezashi ² , Toshinori Tsuru ^{2,*}  and Joji Ohshita ^{1,3,*} 

- ¹ Smart Innovation Program, Graduate School of Advanced Science and Engineering, Hiroshima University, Higashi-Hiroshima 739-8527, Japan; hoza@k-jundai.jp (K.H.); m226478@hiroshima-u.ac.jp (T.Y.)
- ² Chemical Engineering Program, Graduate School of Advanced Science and Engineering, Hiroshima University, Higashi-Hiroshima 739-8527, Japan; kanezashi@hiroshima-u.ac.jp
- ³ Division of Materials Model-Based Research, Digital Monozukuri (Manufacturing) Education and Research Center, Hiroshima University, Higashi-Hiroshima 739-0046, Japan
- * Correspondence: tsuru@hiroshima-u.ac.jp (T.T.); jo@hiroshima-u.ac.jp (J.O.)

Abstract: New polysilsesquioxane (PSQ)-based CO₂ separation membranes with succinic anhydride and monoalkylurea units as thermally degradable CO₂-philic units were prepared by the copolymerization of a 1:1 mixture of [3-(triethoxysilyl)propyl]succinic anhydride (TESPS) or [3-(triethoxysilyl)propyl]urea (TESPU) and bis(triethoxysilyl)ethane (BTESE). The succinic anhydride and monoalkylurea units underwent thermal degradation to form ester and dialkylurea units, respectively, with the liberation of small molecules (e.g., CO₂ and NH₃) under N₂ atmosphere. The effects of thermal degradation on the performance of the obtained membranes were investigated. The TESPS-BTESE- and TESPU-BTESE-based membranes calcined at 250 °C and 200 °C exhibited good CO₂/N₂ permselectivities of 20.2 and 14.4, respectively, with CO₂ permeances of 7.7×10^{-8} and 7.9×10^{-8} mol m⁻²·s⁻¹·Pa⁻¹, respectively. When the membranes were further calcined at elevated temperatures of 350 °C and 300 °C, respectively, to promote the thermal degradation of the organic units, the CO₂ permeances increased to 1.3×10^{-7} and 1.2×10^{-6} mol m⁻²·s⁻¹·Pa⁻¹ (3.9×10^2 and 3.6×10^3 GPU), although the CO₂/N₂ permselectivities decreased to 19.5 and 8.4, respectively. These data indicate that the controlled thermal degradation of the organic units provides a new methodology for possible tuning of the CO₂ separation performance of PSQ membranes.

Keywords: polysilsesquioxane; membrane; CO₂ separation; sol-gel process; thermal degradation



Citation: Horata, K.; Yoshio, T.; Miyazaki, R.; Adachi, Y.; Kanezashi, M.; Tsuru, T.; Ohshita, J. Preparation of Polysilsesquioxane-Based CO₂ Separation Membranes with Thermally Degradable Succinic Anhydride and Urea Units. *Separations* **2024**, *11*, 110. <https://doi.org/10.3390/separations11040110>

Academic Editors: Aatif Ali Shah and Hosik Park

Received: 5 March 2024

Revised: 21 March 2024

Accepted: 24 March 2024

Published: 2 April 2024



Copyright: © 2024 by the authors. Licensee MDPI, Basel, Switzerland. This article is an open access article distributed under the terms and conditions of the Creative Commons Attribution (CC BY) license (<https://creativecommons.org/licenses/by/4.0/>).

1. Introduction

Membrane CO₂ separation is being actively studied as a simple and low-cost CO₂ recovery technology, as the reduction in CO₂ emissions has become an utmost necessity for resolving global warming issues. Many CO₂ separation membranes have been developed, including those based on organic and inorganic materials [1–4]. Mixed-matrix membranes and metal organic framework membranes have also emerged as new classes of CO₂ separation membranes [5,6]. Polysilsesquioxane (PSQ)-based membranes attract recent attention as typical organic–inorganic hybrid membranes because of such characteristics as high processability and durability, being both organic and inorganic materials [7–16]. Of these membranes, ladder-type PSQ-containing films with CO₂-philic units, such as polyethylene oxide chains, have been studied as self-standing CO₂ separation films [7,8]. Membranes with random-type PSQ layers coated on porous supporting substrates have also been studied. For example, a membrane prepared by coating an inorganic support with a PSQ layer, which is prepared from a primary amine

precursor aminopropyltriethoxysilane (APTES: Chart 1) using the sol-gel method, exhibits CO₂ separation properties with CO₂/N₂ permselectivity of 22 and a CO₂ permeance of $2.6 \times 10^{-8} \text{ mol m}^{-2} \cdot \text{s}^{-1} \cdot \text{Pa}^{-1}$ [3,9]. The performance of these membranes is strongly dependent on the structures of CO₂-philic units and can be improved by the use of a tertiary amine precursor *N,N'*-dimethylaminopropyltriethoxysilane (DMAPTES) (CO₂/N₂ permselectivity = 21, CO₂ permeance = $1.72 \times 10^{-7} \text{ mol m}^{-2} \cdot \text{s}^{-1} \cdot \text{Pa}^{-1}$). However, a secondary amine-containing membrane prepared from *N*-methylaminopropyltriethoxysilane (MAPTES) exhibits an inferior performance (CO₂/N₂ = 11, CO₂ permeance = $1.7 \times 10^{-8} \text{ mol m}^{-2} \cdot \text{s}^{-1} \cdot \text{Pa}^{-1}$) [9,10]. Ester units have been reported to possess appropriate CO₂-philicity for CO₂ separation, and by optimizing the monomer ratio, the copolymerization of MeO(C=O)CH₂Si(OEt)₃ and (EtO)₄Si (TEOS) yielded a membrane with a high CO₂ permeance ($2.074 \times 10^{-6} \text{ mol m}^{-2} \cdot \text{s}^{-1} \cdot \text{Pa}^{-1}$) and a moderate CO₂/N₂ permselectivity (7.5) [11]. Polydimethylsiloxane (PDMS)-based materials have been also studied as CO₂ separation membranes [17].

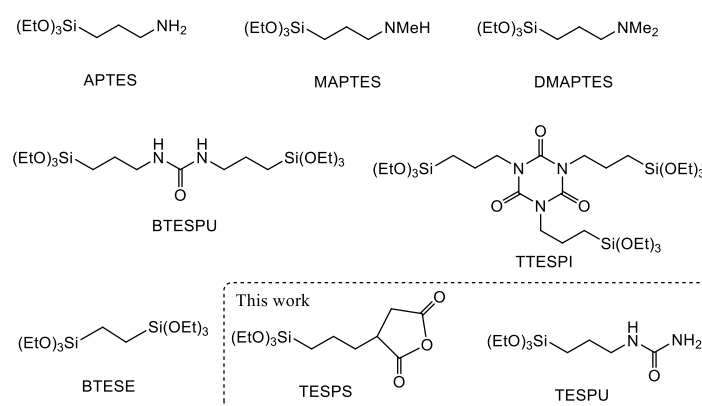


Chart 1. Precursors of PSQ membranes for CO₂ separation.

In general, the higher the CO₂-philicity, the higher the permselectivity; however, an exceedingly high CO₂-philicity may prevent the desorption of CO₂ molecules, hindering the permeation of CO₂ through the membrane, i.e., there is a trade-off relationship between CO₂ permeance and selectivity, two important parameters of CO₂ separation performance. To address this issue, we examined the introduction of urea and isocyanurate groups as units with moderately high CO₂-philicity to the membranes and found that *N,N',N''*-tris(triethoxysilylpropyl)isocyanurate (TTESPI) afforded a membrane with high performance (CO₂/N₂ = 18, CO₂ permeance = $3.2 \times 10^{-7} \text{ mol m}^{-2} \cdot \text{s}^{-1} \cdot \text{Pa}^{-1}$) comparable to the DMAPTES-based membrane (Chart 1) [15]. The CO₂ permeance increased to $5.5 \times 10^{-7} \text{ mol m}^{-2} \cdot \text{s}^{-1} \cdot \text{Pa}^{-1}$ by copolymerization with bis(triethoxysilyl)ethane (BTESE). However, the CO₂/N₂ permselectivity decreased to 12 at the same time. Similarly, the polymerization of *N,N'*-bis(triethoxysilylpropyl)urea (BTESPU) gave a membrane with a lower CO₂ permeance of $3.8 \times 10^{-9} \text{ mol m}^{-2} \cdot \text{s}^{-1} \cdot \text{Pa}^{-1}$, but its 1:1 copolymerization with BTESE gave a membrane with an improved CO₂ permeance of $2.4 \times 10^{-7} \text{ mol m}^{-2} \cdot \text{s}^{-1} \cdot \text{Pa}^{-1}$ from the homopolymer membrane, although the CO₂/N₂ permselectivity decreased from 16 to 13. This is likely due to the dilution of the CO₂-philic urea units in the membrane, demonstrating again the trade-off relationship between the two parameters.

To explore a new strategy to control the performance of PSQ-based CO₂ separation membranes, we designed PSQ precursors with thermally degradable organic units. We anticipated that the thermal degradation of the organic units would generate void spaces by the liberation of small molecules, thereby allowing for the control of PSQ siloxane networks to improve the CO₂ permeance. In this paper, we report the preparation and evaluation of new CO₂ separation membranes containing succinic anhydride as a thermally degradable CO₂-philic unit by the 1:1 copolymerization of [(3-triethoxysilyl)propyl]succinic anhydride (TESPS) and BTESE (Chart 1). The succinic anhydride units were thermally con-

verted into ester units with the release of CO₂ molecules. *N*-[(3-triethoxysilyl)propyl]urea (TESPU) with monoalkylurea as the thermally degradable unit was also examined for use as a PSQ precursor in the copolymerization with BTESE, which involved the formation of a dialkylurea unit from two monoalkylurea units by degradative condensation. The results indicate the possible tuning of the separation properties by controlling the thermal degradation of the organic units of the membranes. The copolymerization of *N*-[(trimethoxysilyl)propyl]urea and TEOS has been reported to generate a membrane with the maximum CO₂/N₂ permselectivity and CO₂ permeance of 6–7 and ca. 4×10^{-7} mol m⁻²·s⁻¹·Pa⁻¹, respectively, at 300 K [16]. However, no study has reported the controlled thermal degradation of the membranes.

2. Materials and Methods

2.1. General

PSQ precursors TESPS, TESPU, and BTESE were purchased from Tokyo Chemical Industry Co., Ltd. (Tokyo, Japan) or Gelest, Inc. (Morrisville, PA, USA), and used as received. Ethanol was distilled from (EtO)₂Mg/EtOH and stored over activated molecular sieves until use. Infrared (IR) spectra were obtained by a Shimadzu IRAffinity-1 spectrophotometer (Shimadzu Corp., Kyoto, Japan). NMR spectra were recorded on a Varian System 500 spectrometer (Agilent Technologies, Inc., Santa Clara, CA, USA). Thermogravimetric analysis (TGA) was performed using an SII TG/DTA-6200 analyzer (Seiko Instruments Inc., Chiba, Japan) under a gentle nitrogen flow (30 mL/min) at a heating rate of 10 °C/min. The TG-mass spectrometry (TG-MS) analysis was carried out on a JEOL Q1500 spectrometer (JEOL, Ltd., Akishima, Japan) equipped with a NETZSCH STA 449 F1 TG/DTA thermal analyzer. Dynamic light scattering (DLS) measurements were carried out on a Malvern Zetasizer Nano ZS analyzer. Scanning Electron Microscope (SEM) images were obtained on a Hitachi S-4800 SEM.

2.2. Membrane Preparation and Gel Characterization

The sol formation was carried out as previously reported for the preparation of urea- and isocyanurate-containing polysilsesquioxane membranes [15]. In a 50 mL glass vial, an ethanol solution of 1:1 weight ratio mixture of TESPS-BTESE or TESPU-BTESE was placed, and water was slowly added to the stirred mixture while stirring at room temperature. The vial was tightly sealed with a screw cap and further stirred until the mean sol particle size reached 2–3 nm (Figure S1). The amounts of reagents and ethanol, and the reaction times for the formation of TESPS-BTESE and TESPU-BTESE sols are listed in Table 1 (runs 1 and 2, respectively). The resultant sols were diluted by adding ethanol to 0.25 wt% based on the monomer contents, and were stored in a refrigerator (4 °C) until use. For nitrogen adsorption isotherm measurements and TGA, the sols were heated to 60 °C in air to generate the gel powders. For IR analysis, the sols were coated on KBr plates and the plates were dried at 50 °C. After heating the coated plates for 10 min at different temperatures, the plates were subjected to IR measurements.

Table 1. Sol formation from TESPS-BTESE and TESPU-BTESE.

Run	Precursor /g (/mmol)	BTESE /g (/mmol)	Ethanol /g	Water /g (/mmol)	Reaction Time/h
1	TESPS 0.30 (0.99)	0.30 (0.85)	7.43	3.30 (183)	48
2	TESPU 0.31 (1.2)	0.30 (0.85)	7.11	4.28 (238)	96

For the preparation of the support membrane [18], a commercially available α -alumina porous tubular substrate (10 mm ϕ , average pore size = 1 μ m) was coated with an aqueous colloidal sol containing large and small α -alumina particles with average sizes of 1.9 μ m and 0.2 μ m, respectively, and the coated substrate was heated at 200 °C for 10 min and then at 550 °C for 10 min in air. The surface of the resultant alumina substrate was coated

with silica–zirconia aqueous sols with different particle sizes in the order of 20–30 nm sol (1 wt%), 10–14 nm sol (0.5 wt%), and 4–10 nm sol (0.5 wt%), and the intermediate layer with a pore size of ca. 1.5 nm was formed by calcination at 550 °C for 10 min in air. The intermediate layer was coated by the PSQ sols and the coated substrates were calcined at different temperatures to produce separation membranes. The coating–calcination process was repeated 2–3 times until the He/SF₆ permselectivity at 200 °C exceeded 1000 or the SF₆ permeance became lower than $1.0 \times 10^{-9} \text{ mol m}^{-2} \cdot \text{s}^{-1} \cdot \text{Pa}^{-1}$. Membrane characterization and the evaluation of gas separation performance were carried out as reported previously [19]. The gas permeability P was obtained along the equation of $P = V/(22.4 \times A \times \Delta P)$, where ΔP is the pressure difference between the upstream and downstream sides of the membrane, V is the flow rate, and A is the membrane surface. Pure gas was supplied to the membrane module under a pressure of approximately 100 kPa at various temperatures of 200 °C, 150 °C, 100 °C, and 50 °C.

2.3. Quantum Chemical Calculations

All quantum chemical calculations were performed on a Gaussian 16 program package (Gaussian, Inc., Wallingford, CT, USA) at the B3LYP/6-31G level of theory. Coordination energies were calculated by subtracting the heat of formation of CO₂ and a precursor model from that of the corresponding complex in the gas phase. Zero-point energies were included in the calculations.

3. Results and Discussion

3.1. Design of CO₂-Philic Groups

The formation of 1:1 complexes of a CO₂ molecule and trimethylsilylpropylsuccinic anhydride (i.e., model of TESPS) was investigated by DFT calculations at the B3LYP/6-31G level, revealing three thermodynamically stable complexes with different kinds of interactions (Types I–III), as shown in Figure 1. In Type I complex, the CO₂ carbon atom is chelated by the carbonyl and ether oxygens of the succinic anhydride unit, whereas in Type II complex, there is only a single site interaction between the CO₂ carbon atom and one of the succinic anhydride carbonyl oxygens. A coordination through the chelate interaction between the CO₂ oxygen and anhydride carbonyl carbons is observed in a Type III complex. The coordination energy of CO₂ to succinic anhydride was calculated to be approximately –12 kJ/mol for each complex formation.

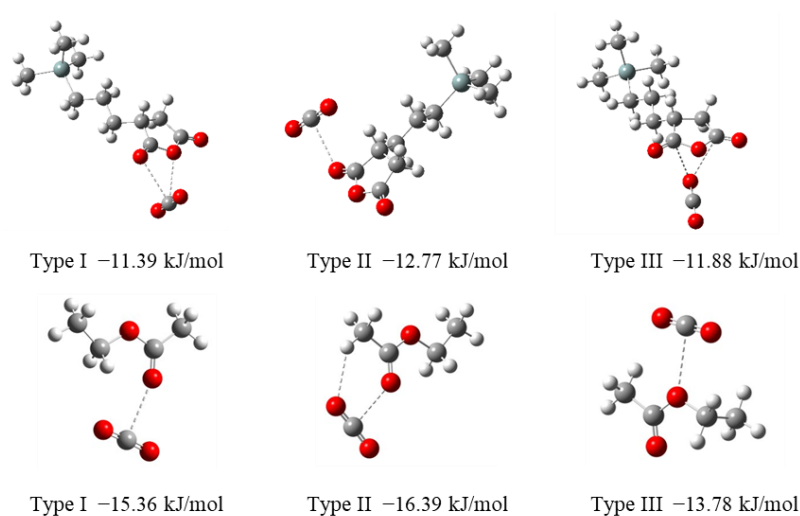


Figure 1. Optimized geometries of the complexes of CO₂ and TESPS/ester models.

The coordination energies of CO₂ to ethyl acetate, a model of the ester unit that would be formed by the thermal degradation of succinic anhydride in PSQ (vide infra), were also calculated and were found to have larger negative value than those of the succinic

anhydride model (Figure 1). In Type I–III complexes, a CO₂ molecule interacts with the carbonyl or ether oxygen of ethyl acetate at the central carbon atom. The formation of the Type II complex involves the interaction between the alkyl C–H unit and the CO₂ oxygen atom, as reported for the formation of a methyl acetate–CO₂ complex [20]. On the other hand, the coordination energy of CO₂ to *N,N'*-diethylurea (i.e., model of TESPU), which involves a chelate-type interaction as presented in Chart 2, was previously computed to be approximately -28 kJ/mol [15].

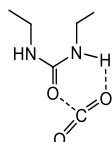


Chart 2. Coordination of CO₂ to *N,N'*-diethylurea.

3.2. Membrane Preparation

The sols prepared by the hydrolysis/condensation of the precursors in ethanol were coated on the intermediate layer of the support membrane and calcined in nitrogen to produce the PSQ gel layers, as shown in Figure 2. The calcination temperature was determined on the basis of the IR spectra measured after heating at each temperature for 10 min and the results of TGA, as shown in Figures 3 and 4, respectively. The TGA of the gels prepared from TESPS-BTESE and TESPU-BTESE revealed no significant weight loss up to 200 °C, with a gradual decrease thereafter up to 700 °C.

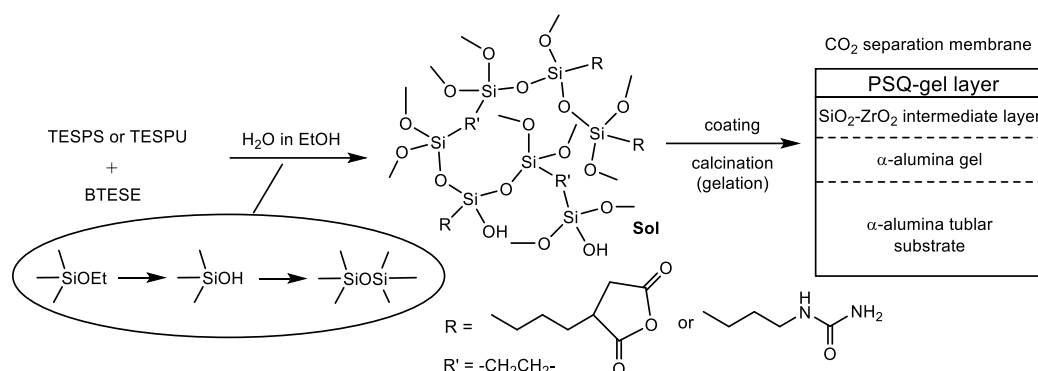


Figure 2. Membrane preparation.

For the TESPS-BTESE gel, the IR spectrum obtained after heating at 50 °C showed a carbonyl signal at 1715 cm^{-1} with a shoulder at 1738 cm^{-1} , as shown in Figure 3a. These signals, which were too low in energies to be assigned as succinic anhydride signals, are attributable to the ester or carboxylic acid unit with and without hydrogen bonding, respectively. The hydrogen bonding was probably formed intramolecularly and intermolecular hydrogen bonding with water, ethanol, and silanol units would be also involved when calcined at this temperature. On the basis of the IR spectrum, it is likely that the succinic anhydride unit underwent reactions with ethanol or water under hydrolysis/condensation conditions to provide, unexpectedly, a ring-opened ester or a carboxylic acid unit. It is likely that the silanol (Si–OH) unit, which was formed by the hydrolysis of the ethoxy–Si bond, acted as a weak acid catalyst for the hydrolysis of the succinic anhydride unit. Indeed, the ¹³C NMR spectrum of the mixture of TESPS-BTESE revealed multiple carbonyl carbon signals at 173–178 ppm after treatment with water in ethanol, as shown in Figure 5. These signals were low-field sifted from those of TESPS in accordance with the fact that succinic acid and diethyl succinate show the signals at 179.9 ppm and 172.4 ppm, respectively, lower than that of succinic anhydride (170.7 ppm). From 150 °C to 250 °C, the 1715 cm^{-1} peak gradually decreased in intensity and a new peak at 1783 cm^{-1} , likely due to the succinic anhydride unit, appeared. However, the succinic anhydride peak that appeared

at 1783 cm^{-1} was weakened at $300\text{ }^{\circ}\text{C}$ and disappeared at $350\text{ }^{\circ}\text{C}$. During this process, the signal at 1738 cm^{-1} , which was observed as a shoulder from $50\text{ }^{\circ}\text{C}$ to $200\text{ }^{\circ}\text{C}$ and attributable to the ester or carboxylic acid unit without hydrogen bonding, appeared as a sharp peak at $250\text{ }^{\circ}\text{C}$, but became broad at $350\text{ }^{\circ}\text{C}$ and weakened at $400\text{ }^{\circ}\text{C}$. A broad peak centered at 3300 cm^{-1} , which corresponds to the O–H stretching of water, carboxylic acid, and/or silanol, almost disappeared at $250\text{ }^{\circ}\text{C}$. At the same time, the Si–OH vibration band around 900 cm^{-1} decreased in intensity as the heating temperature increased, suggesting the formation of siloxane linkages by the condensation of the silanol units. However, the Si–OH band was observed even at $400\text{ }^{\circ}\text{C}$, although the intensity was low.

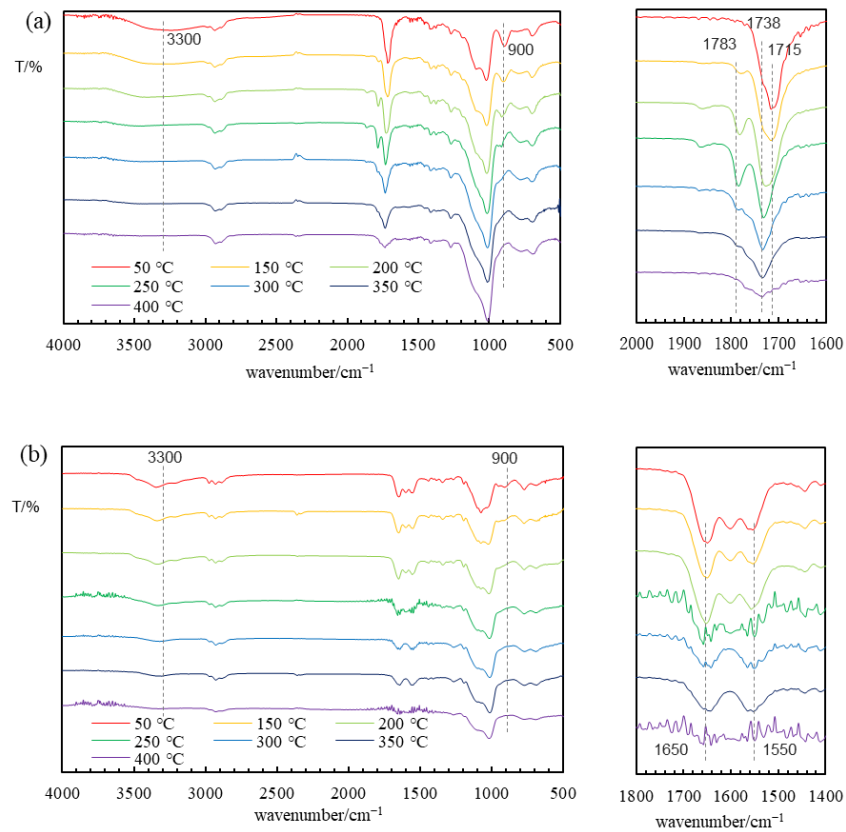


Figure 3. IR spectra of TESPS-BTESE- (a) and TESPU-BTESE- (b) based gel films on KBr plates after heating at different temperatures in nitrogen, with expansions of spectra for C=O stretching and N–H bending vibrations (for TESPU-BTESE).

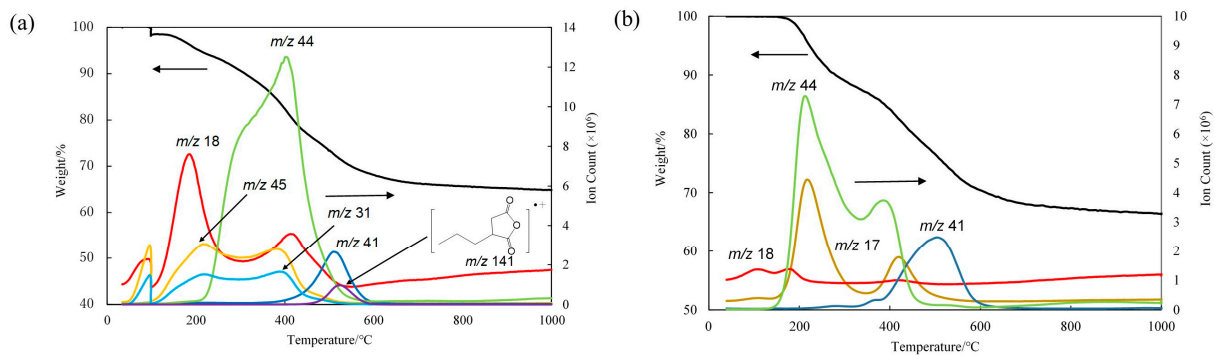


Figure 4. TG and TG-MS profiles of TESPS-BTESE (a) and TESPU-BTESE (b) gels in nitrogen at a heating rate of $10\text{ }^{\circ}\text{C}/\text{min}$. Arrows indicate the corresponding axes.

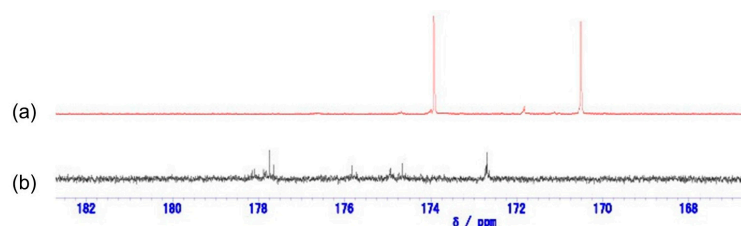


Figure 5. ¹³C NMR spectra of (a) TESP and (b) a mixture of TESP-BTESE after treatment with water/ethanol in CDCl₃, showing the carbonyl signals.

To obtain more information about this process, we carried out a TG-MS analysis of the gels, as shown in Figure 4a. The TG-MS profiles of the TESP-BTESE gel revealed the formation of water (*m/z* 18), ethanol (*m/z* 45 and 31), and CO₂ (*m/z* 44) at elevated temperatures (Figure 4a). On the basis of these spectral observations, we speculated that the ring-opened products underwent ring closure at temperatures higher than 150 °C (Figure 6b). Thermal decarbonylation also occurred at temperatures higher than 250 °C, giving ethyl ester and/or carboxylic acid units, which might react with silanol units to produce silyl ester units. The ethyl ester units seemed to be thermally stable even at a high temperature. In fact, related poly(ethyl acrylate) is known to be stable up to 300 °C, and only an approximately 9% weight loss was observed by TGA in nitrogen [21]. The ethyl ester units might remain at high temperatures unless they reacted with silanol units. The decomposition of the acid anhydride units observed at 300 °C was likely due to the reaction with the silanol units, followed by spontaneous decarbonylation, yielding silyl ester units, since it did not appear that large amounts of other nucleophiles such as water and ethanol remained in the gel at high temperatures. The TG-MS profiles also revealed a small peak at *m/z* 141, which corresponds to a fragment containing a succinic anhydride unit, at 300 °C or higher temperatures, indicating that the succinic anhydride units were not all degraded but remained to some extent. An unidentified peak of *m/z* 41 was observed at temperatures higher than 390 °C.

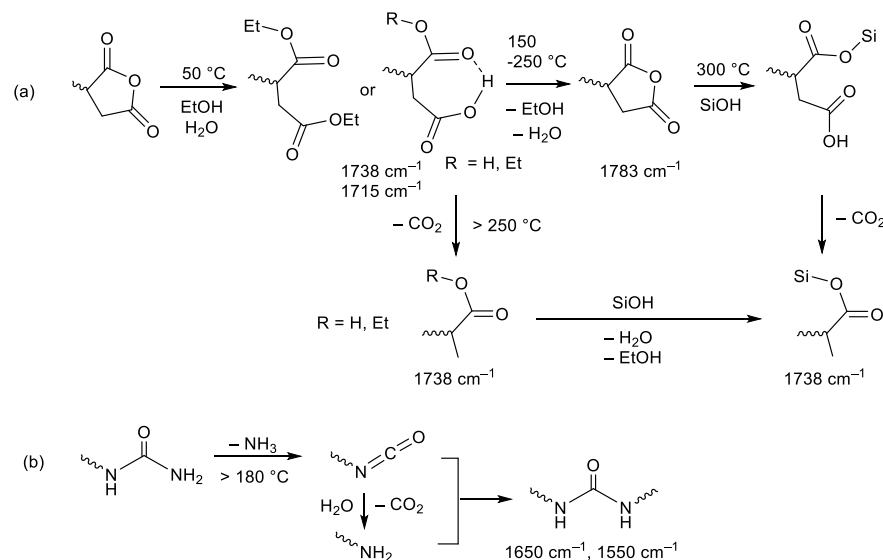


Figure 6. Mechanistic interpretation of the thermal degradation of succinic anhydride (a) and the urea (b) units of TESP-BTESE- and TESP-BTESE-based membranes.

The IR spectrum of the TESP-BTESE-based gel film prepared on a KBr plate showed three peaks at 1500–1700 cm⁻¹, which are characteristic of the monosubstituted urea units. These peaks were broadened after heating at 250 °C, and two peaks at 1650 cm⁻¹ and 1550 cm⁻¹ due to C=O stretching and N–H bending vibrations, respectively, were observed in the spectrum after heating at 300 °C (Figure 3b). The signals at 1650 cm⁻¹

and 1550 cm^{-1} closely resembled those of the IR spectrum of the BTESPU gel [15] and were assignable to N,N' -disubstituted urea units. The signals of the N,N' -disubstituted urea units remained unchanged after heating at $350\text{ }^{\circ}\text{C}$. The silanol signal at 900 cm^{-1} decreased in intensity by heating at $150\text{ }^{\circ}\text{C}$ and $200\text{ }^{\circ}\text{C}$, with no further decrease at higher temperatures. The vibration peak of O–H/N–H bonds around 3300 cm^{-1} also decreased, but did not disappear after heating at $350\text{ }^{\circ}\text{C}$. The TG-MS analysis of the TESPU-BTESE gel revealed that NH_3 and CO_2 are formed at temperatures higher than $180\text{ }^{\circ}\text{C}$ (Figure 4b). A possible mechanistic interpretation of this phenomenon is presented in Figure 6b. It is known that monosubstituted urea undergo thermal degradation to form isocyanate with the liberation of NH_3 [22,23]. The hydrolysis of the isocyanate unit with water results in the formation of amine and CO_2 . Thus-formed amine reacts with the isocyanate unit to form the N,N' -disubstituted urea unit. An unidentified peak of m/z 41 was observed in the TG-MS of TESPU-BTESE-based gels at temperatures higher than $390\text{ }^{\circ}\text{C}$, similarly to that of TESPS-BTESE.

On the basis of these results, we examined the CO_2 separation performance of the membranes calcined at different temperatures to observe the effects of the thermal degradation of the CO_2 -philic units. The TESPS-BTESE films were calcined at $250\text{ }^{\circ}\text{C}$ and $300\text{ }^{\circ}\text{C}$, at which the succinic anhydride unit reformation and the ester unit formation would complete, respectively. Calcination at $350\text{ }^{\circ}\text{C}$ was also examined for TESPS-BTESE. For TESPU-BTESE, the membranes prepared by calcination at $200\text{ }^{\circ}\text{C}$ and $300\text{ }^{\circ}\text{C}$ were investigated, because the monoalkylurea units seemed to be converted to dialkylurea units between $200\text{ }^{\circ}\text{C}$ and $300\text{ }^{\circ}\text{C}$. The membrane calcined at $300\text{ }^{\circ}\text{C}$ showed a largely decreased CO_2/N_2 permselectivity from that calcined at $200\text{ }^{\circ}\text{C}$ (vide infra), and calcination at higher temperature was not examined for TESPU-BTESE. The gels obtained from TESPS-BTESE and TESPU-BTESE were not porous according to the nitrogen adsorption analysis, regardless of the calcination temperature, as shown in Figure S2. However, void spaces would be formed in the PSQ layers by the thermal degradation of the organic units, affecting the CO_2 separation properties of the membranes.

3.3. Gas Permeation

The pure gas permeance data of the TESPS-BTESE- and TESPU-BTESE-based PSQ membranes calcined at different temperatures are shown in Figure 7. The SF_6 permeation of the TESPS-BTESE-based membrane calcined at $250\text{ }^{\circ}\text{C}$ (TESPS-BTESE(250)) was too slow to determine the permeance. The plots of the gas permeance of the membranes vs. the kinetic diameter of gas molecules from N_2 to SF_6 had larger negative slopes than the Knudsen plots, as shown in Figure 7, suggesting the molecular sieving effects of the membranes for gas separation in this region. Figure 8 shows the SEM cross-sections of the TESPS-BTESE membranes calcined at different temperatures on the inorganic support. The TESPS-BTESE (250) membrane showed some gaps on the surface, which became smooth as the calcination temperature was elevated, and the TESPS-BTESE(350) membrane showed an almost flat surface. It was found that all the membranes possessed no defects such as cracks and pinholes on the surface. As the boundary of the PSQ and intermediate layers could not be clearly seen, we could not determine the thicknesses of the PSQ separation layers.

The CO_2 permeances and CO_2/N_2 permselectivities of the membranes at $50\text{ }^{\circ}\text{C}$ are summarized in Table 2. Figure 9 shows the trade-off plots of CO_2 permeance vs. CO_2/N_2 permselectivity of the membranes prepared in the present study, together with those of previously reported PSQ-based membranes. For both TESPS-BTESE- and TESPU-BTESE-based membranes, gas permeance increased with an increasing calcination temperature, possibly due to the enhanced siloxane network formation and the thermal degradation of the organic units; the former decreases the number of silanol groups that hinder the gas permeation in terms of the steric hindrance and CO_2 -philicity, whereas the latter lowers the membrane density by the formation of void spaces, although the gels were found to be non-porous in the nitrogen adsorption analysis regardless of the calcination temperature as mentioned above. The trade-off relationship between CO_2 permeance and

CO₂/N₂ permselectivity is generally observed for CO₂ separation membranes [1]. However, the TESPS-BTESE-based membranes showed only slight decreases in permselectivity; increasing the calcination temperature from 250 °C to 350 °C resulted in an increase in the CO₂ permeance of the TESPS-BTESE-based membrane (TESPS-BTESE(350)) by 1.7-fold compared with that of TESPS-BTESE(250), with an almost negligible decrease in CO₂/N₂ permselectivity from 20.2 to 19.5, overcoming the general trade-off relationship between the CO₂ permeance and CO₂/N₂ permselectivity. This can be understood from the higher CO₂-philicity of the ester unit than the acid anhydride unit, as suggested by DFT calculations (vide supra). We also examined the CO₂ separation properties of PSQ membranes prepared by the homopolymerization of TESPS; however, the membranes consistently showed lower CO₂ permeances and CO₂/N₂ permselectivities than the TESPS-BTESE-based membranes (Table 2). The membranes were found to be durable and standing the membranes at 200 °C for 5 days resulted in no obvious changes of the CO₂ permeances and CO₂/N₂ permselectivities.

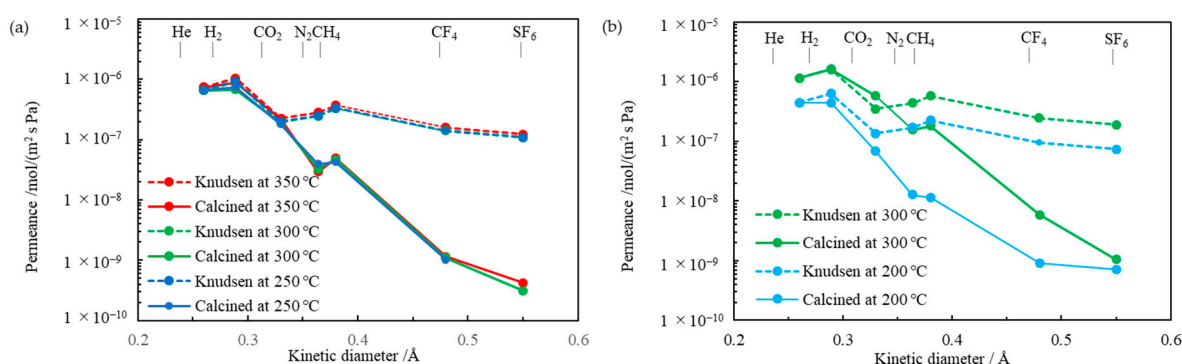


Figure 7. Comparison of pure gas permeance at 200 °C for (a) TESPS-BTESE- and (b) TESPU-BTESE-based membranes calcined at different temperatures, together with Knudsen plots estimated from the helium permeance data for each membrane.

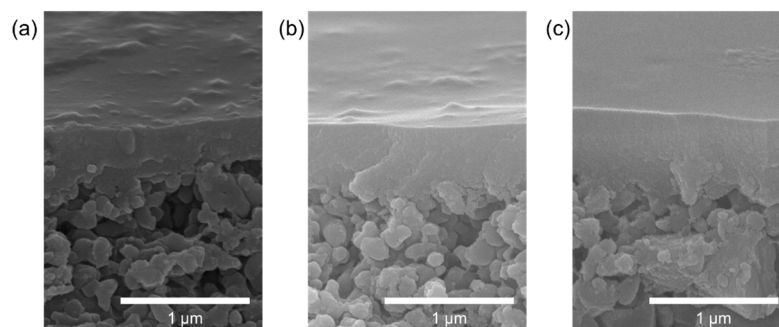


Figure 8. SEM cross-sections of TESPS-BTESE membranes calcined at (a) 250 °C (b) 300 °C, and (c) 350 °C, respectively.

The CO₂ permeance of the TESPU-BTESE-based membranes markedly increased with the increasing calcination temperature, although a decrease in CO₂/N₂ permselectivity was noted at the same time. This indicates that the TESPU-BTESE-based membranes behave as predicted by the trade-off relationship. A highly CO₂-permeable membrane was obtained when calcined at a high temperature (TESPU-BTESE(300)), with a somewhat low CO₂/N₂ permselectivity of 8.4. Interestingly, the PSQ membrane obtained by the 1:1 copolymerization of BTESPU-BTESE having *N,N'*-disubstituted urea units [15], similar to TESPU-BTESE(300), had a much lower CO₂ permeance than TESPU-BTESE(300). This could be due to the decreased number of CO₂-philic urea units in TESPU-BTESE(300), because one *N,N'*-disubstituted urea unit is formed from two monosubstituted urea units by thermal degradation (Figure 6b). However, the membrane prepared by the 1:2 copolymerization

of BTESPU-BTESE showed a similar performance to the membrane prepared by the 1:1 copolymerization (Figure 9) [15]. Thus, factors other than the chemical transformation of the CO₂-philic units—void space formation, for example—may be operative in TESPU-BTESE(300), affecting the CO₂ separation performance.

Table 2. Properties of TESPS-BTESE- and TESPU-BTESE-based membranes and those of previously reported urea- and isocyanurate-containing PSQ membranes.

Precursor	Calcination Temp/°C	CO ₂ Permeance /mol m ⁻² ·s ⁻¹ ·Pa ⁻¹	CO ₂ /N ₂ ¹	E _{act} /kJmol ⁻¹ ²	
				CO ₂	N ₂
TESPS-BTESE (1:1)	250	7.7 × 10 ⁻⁸	20.2	7.3	17.2
	300	8.9 × 10 ⁻⁸	19.3	6.4	14.7
	350	1.3 × 10 ⁻⁷	19.5	4.5	10.3
TESPU-BTESE (1:1)	200	7.9 × 10 ⁻⁸	14.4	-1.3	7.1
	300	1.2 × 10 ⁻⁶	8.4	-6.4	0.5
TESPS	250	4.8 × 10 ⁻⁹	9.4	27.5	31.0
	300	6.4 × 10 ⁻⁹	2.2	24.1	21.2
	350	1.2 × 10 ⁻⁷	11.5	11.5	17.7
BTESPU-BTESE (1:1) ³	300	2.2 × 10 ⁻⁷	13	0.3	9.1
BTESPU-BTESE (1:2) ³	300	2.0 × 10 ⁻⁷	13	0.35	10.1
TTESPI ³	300	3.2 × 10 ⁻⁷	18	3.3	14.4
TTESPI-BTESE (1:1) ³	300	5.5 × 10 ⁻⁷	12	-2.5	4.9

¹ Permselectivity at 50 °C. ² Activation energies based on the slopes of gas permeance-1/T plots. For the present membranes, see Figure S3. ³ Data from reference [15].

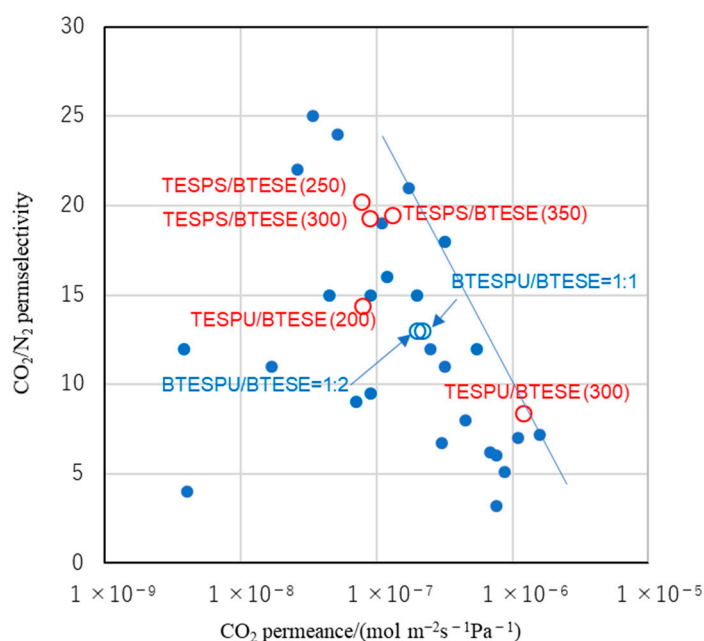


Figure 9. Performance of PSQ-based CO₂ separation membranes prepared in the present study (red) and those prepared in our previous study (blue). Numbers in parentheses indicate calcination temperatures. A solid line is drawn as a guide of the trade-off upper limit of the previously reported PSQ-based membranes.

To learn more about the separation performance of the membranes, we determined their temperature-dependent gas permeances, as presented in Figure S3. Based on these

data, activation energies were calculated for each gas, as summarized in Table S1; those of CO₂ and N₂ are also listed in Table 2. The TESPS-BTESE-based membranes showed higher activation energies than the TESPU-BTESE-based membranes for all gases, suggesting the higher network rigidity of the TESPU-BTESE-based membranes. This may be partly due to the urea–urea interaction by hydrogen bonding, particularly for the TESPU-BTESE-based membrane with NH₂ units calcined at 200 °C (TESPU-BTESE(200)). Hydrogen bonding between the urea units in the PSQ membranes prepared from BTESPU has been reported previously [15]. Calcination at a higher temperature (TESPU-BTESE(300)) led to even lower activation energies, likely due to an increase in structural rigidity by the enhanced network formation and the conversion of the monoalkylurea units into the dialkylurea units. Void space formation by the thermal degradation of the monoalkylurea units may also be a reason for the low activation energies. TESPS homopolymer membranes exhibited higher activation energies than the TESPS-BTESE-based membranes, suggesting the effects of the BTESE-derived units in the membranes enhancing the network rigidity.

The activation energies for the CO₂ permeation of the membranes prepared in the present study were lower than those for N₂ permeation, despite their similar molecular sizes, indicating the adsorption-controlled mechanism for CO₂ separation by these membranes, as observed for other amine, urea, and isocyanurate-containing PSQ membranes reported previously [9,14,15]. The low activation energies for the CO₂ permeation of the TESPU-BTESE-based membranes compared with those of the TESPS-BTESE-based membranes are in line with the higher network rigidity of the TESPU-BTESE-based membranes. The higher CO₂-philicity of the urea unit than the ester unit may also be the reason for the lower activation energies for the CO₂ permeation of the TESPU-BTESE-based membranes (Figure 1 and Chart 2).

4. Conclusions

The TESPS-BTESE- and TESPU-BTESE-based CO₂ separation membranes were prepared by the sol–gel method, and the effects of the thermal degradation of the organic units on membrane performance were investigated, revealing the possibility of tuning the separation properties by controlling thermal degradation following membrane formation. The degradation process was examined by means of TG-MS and temperature-dependent IR spectra, and the CO₂ separation mechanism was investigated in terms of activation energies. Among the PSQ-based CO₂ separation membranes prepared in the present study, TESPS-BTESE(350) and TESPU-BTESE(300) exhibited the CO₂ permeance and CO₂/N₂ permselectivity near the trade-off upper limit. Although the performance of these membranes was not very high compared with other types of membranes including organic polymer membranes and mixed-matrix membranes (Figure S4), their high processability and thermal stability are advantageous for use as PSQ membranes. The high CO₂ permeance of TESPU-BTESE(300) is also noteworthy.

Supplementary Materials: The following supporting information can be downloaded at: <https://www.mdpi.com/article/10.3390/separations11040110/s1>, Figure S1: Progress of sol formation from TESPS/BTESE (a) and TESPU/BTESE (b) 1/1 mixtures monitored by DLS measurements at different reaction times; Figure S2: Nitrogen adsorption isotherms for TESPS/BTESE and TESPU/BTESE gels; Figure S3: Temperature-dependent gas permeances of TESPS/BTESE and TESPU/BTESE membranes calcined at different temperatures; Table S1: Activation energies for gas permeation of TESPS/BTESE and TESPU/BTESE membranes.

Author Contributions: Conceptualization, K.H., Y.A., M.K., T.T. and J.O.; methodology, K.H., Y.A., M.K., T.T. and J.O.; investigation, T.Y. and R.M.; data curation, T.Y. and R.M.; quantum chemical calculations, K.H.; writing—original draft preparation, K.H.; writing—review and editing, M.K., T.T. and J.O.; supervision, T.T. and J.O.; project administration, J.O. All authors have read and agreed to the published version of the manuscript.

Funding: This research received no external funding.

Data Availability Statement: Data are contained within the article.

Conflicts of Interest: The authors declare no conflicts of interest.

References

1. Robeson, L.M. The Upper Bound Revisited. *J. Membr. Sci.* **2008**, *320*, 390–400. [[CrossRef](#)]
2. Brunetti, A.; Scura, F.; Barbieri, G.; Drioli, E. Membrane Technologies for CO₂ Separation. *J. Membr. Sci.* **2010**, *359*, 115–125. [[CrossRef](#)]
3. Ma, C.; Wang, M.; Wang, Z.; Gao, M.; Wang, J. Recent Progress on Thin Film Composite Membranes for CO₂ Separation. *J. CO₂ Util.* **2020**, *42*, 101296. [[CrossRef](#)]
4. Dai, Y.; Niu, Z.; Luo, W.; Wang, Y.; Mu, P.; Li, J. A Review on the Recent Advances in Composite Membranes for CO₂ Capture Processes. *Sep. Purif. Technol.* **2023**, *307*, 122752. [[CrossRef](#)]
5. Tien-Binh, N.; Rodrigue, D.; Kliaguine, S. In-situ Cross Interface Linking of PIM-1 polymer and UiO-66-NH₂ for Outstanding Gas Separation and Physical Aging Control. *J. Membr. Sci.* **2018**, *548*, 429–438. [[CrossRef](#)]
6. Duan, K.; Wang, J.; Zhang, Y.; Liu, J. Covalent Organic Frameworks (COFs) Functionalized Mixed Matrix Membrane for Effective CO₂/N₂ Separation. *J. Membr. Sci.* **2019**, *572*, 588–595. [[CrossRef](#)]
7. Woo, R.K.; Lee, A.S.; Park, S.-H.; Baek, K.-Y.; Lee, K.B.; Lee, S.-H.; Lee, J.-H.; Hwang, S.S.; Lee, J.S. Free-standing, Polysilsesquioxane-based Inorganic/organic Hybrid Membranes for Gas Separations. *J. Membr. Sci.* **2015**, *475*, 384–394.
8. Park, S.; Lee, A.S.; Do, Y.S.; Hwang, S.S.; Lee, Y.M.; Lee, J.-H.; Lee, J.S. Rational Molecular Design of PEOlated Ladder-structured Polysilsesquioxane Membranes for High Performance CO₂ Removal. *Chem. Commun.* **2015**, *51*, 15308–15311. [[CrossRef](#)]
9. Yu, L.; Kanezashi, M.; Nagasawa, H.; Tsuru, T. Role of Amine Type in CO₂ Separation Performance within Amine Functionalized Silica/Organosilica Membranes: A Review. *Appl. Sci.* **2018**, *8*, 1032. [[CrossRef](#)]
10. Yu, L.; Kanezashi, M.; Nagasawa, H.; Tsuru, T. Fabrication and CO₂ Permeation Properties of Amine-silica Membranes Using a Variety of Amine Types. *J. Membr. Sci.* **2017**, *541*, 447–456. [[CrossRef](#)]
11. Karimi, S.; Korelskiy, D.; Mortazavi, Y.; Khodadadi, A.A.; Sardar, K.; Esmaeili, M.; Antzutkin, O.N.; Shah, F.U.; Hedlund, J. High Flux Acetate Functionalized Silica Membranes Based on In-situ Co-condensation for CO₂/N₂ Separation. *J. Membr. Sci.* **2016**, *520*, 574–582. [[CrossRef](#)]
12. Xomeriakis, G.; Tsai, C.-Y.; Brnker, C.J. Microporous Sol-gel Derived Aminosilicate Membrane for Enhanced Carbon Dioxide Separation. *Sep. Purif. Technol.* **2005**, *42*, 249–257. [[CrossRef](#)]
13. Paradis, G.G.; Kreiter, R.; van Tuel, M.M.; Nijmeijer, A.; Vente, J.F. Amino-Functionalized Microporous Hybrid Silica Membranes. *J. Mater. Chem.* **2012**, *22*, 7258–7264. [[CrossRef](#)]
14. Ohshita, J.; Okonogi, T.; Kajimura, K.; Horata, K.; Adachi, Y.; Kanezashi, M.; Tsuru, T. Preparation of Amine- and Ammonium-containing Polysilsesquioxane Membranes for CO₂ Separation. *Polym. J.* **2022**, *54*, 875–882. [[CrossRef](#)]
15. Kajimura, K.; Horata, K.; Adachi, Y.; Kanezashi, M.; Tsuru, T.; Ohshita, J. Preparation of Urea- and Isocyanurate-containing Polysilsesquioxane Membranes for CO₂ Separation. *J. Sol-Gel Sci. Technol.* **2023**, *106*, 149–157. [[CrossRef](#)]
16. Karimi, S.; Mortazavi, Y.; Khodadadi, A.A.; Holmgren, A.; Korelskiy, D.; Hedlund, J. Functionalization of Silica Membranes for CO₂ Separation. *Sep. Purif. Technol.* **2020**, *235*, 116207. [[CrossRef](#)]
17. Basu, S.; Khan, A.L.; Cano-Odena, A.; Liu, C.; Vankelecom, I.F.J. Membrane-based Technologies for Bbiogas Separations. *Chem. Rev.* **2010**, *39*, 750–768.
18. Tsuru, T.; Nakasuji, T.; Oka, M.; Kanezashi, M.; Yoshioka, T. Preparation of Hydrophobic Nanoporous Methylated SiO₂ Membranes and Application to Nanofiltration of Hexane Solutions. *J. Membr. Sci.* **2011**, *384*, 149–156. [[CrossRef](#)]
19. Xu, R.; Wang, J.H.; Kanezashi, M.; Yoshioka, T.; Tsuru, T. Reverse Osmosis Performance of Organosilica Membranes and Comparison with the Pervaporation and Gas Permeation Properties. *AIChE J.* **2013**, *59*, 1298–1307. [[CrossRef](#)]
20. Raveendran, P.; Wallen, S. Cooperative C-H...O Hydrogen Bonding in CO₂-Lewis Base Complexes: Implications for Solvation in Supercritical CO₂. *J. Am. Chem. Soc.* **2001**, *124*, 12590–12599. [[CrossRef](#)]
21. McNeil, I.C.; Mohammad, M.H. A Comparison of the Thermal Degradation Behavior of Ethylene-ethyl Acrylate Copolymer, Low Density polyethylene and Poly(ethyl acrylate). *Polym. Degrad. Stab.* **1995**, *48*, 175–187. [[CrossRef](#)]
22. Schaber, P.M.; Colson, T.; Higgins, S.; Thielen, D.; Anspach, B.; Brauer, J. Thermal Decomposition (Pyrolysis) of Urea in an Open Reaction Vessel. *Thermochim. Acta* **2004**, *424*, 131–142. [[CrossRef](#)]
23. Honorien, J.; Fournet, R.; Gaude, P.-A.; Sirjean, B. Theoretical Study of the Thermal Decomposition of Urea Derivatives. *J. Phys. Chem. A* **2022**, *126*, 6264–6277. [[CrossRef](#)] [[PubMed](#)]

Disclaimer/Publisher’s Note: The statements, opinions and data contained in all publications are solely those of the individual author(s) and contributor(s) and not of MDPI and/or the editor(s). MDPI and/or the editor(s) disclaim responsibility for any injury to people or property resulting from any ideas, methods, instructions or products referred to in the content.